SIGMA: Sequence Index Grouping-based Multiple Access for 6G OFDM-ISAC Systems in Multipath Environments

Ha-Eun Lee, Young-Seok Lee, Howon Lee†, and Bang Chul Jung†
Department of Artificial Intelligence Convergence Network, Ajou University, Suwon, 16499, South Korea
†Department of Electrical and Computer Engineering, Ajou University, Suwon, 16499, South Korea
Email: {haeunlee; youngseoklee; howon; bcjung}@ajou.ac.kr

2026 IEEE 23rd Consumer Communications & Networking Conference (CCNC) | 979-8-3315-9673-6/26/$31.00 ©2026 IEEE | DOI: 10.1109/CCNC65079.2026.11366534

***Abstract*—In this paper, we propose a novel sequence index grouping-based multiple access (SIGMA) technique for multi-user orthogonal frequency division multiplexing-based integrated sensing and communication (OFDM-ISAC) systems. The proposed technique ensures collision-free access by performing a pre-assignment of orthogonal sequences (OSs) between the base station (BS) and each user equipment (UE), where each UE modulates its communication data onto the allocated sequence index and transmits it to the BS. By exploiting the autocorrelation property of the received sequences, the BS estimates the distance to each UE, while the direction of each user is obtained using a uniform linear array (ULA) antenna equipped at the BS. Furthermore, to achieve accurate localization even in non-line-of-sight (NLoS) multipath environments, a clustering algorithm and an oversampling technique are incorporated. Extensive simulation results demonstrate that the proposed system achieves robust localization and communication performance in multi-user scenarios.**

***Index Terms*—6G, Multiple access, Orthogonal frequency division multiplexing (OFDM), Integrated sensing and communication (ISAC), Wireless localization.**

I. Introduction

Sixth-generation (6G) communication systems are required to support high-capacity features, such as massive connectivity and ultra-reliable communication, which necessitates a wider frequency spectrum [1]. To address these challenges, integrated sensing and communication (ISAC) is emerging as a pivotal technology for future wireless networks [2]. ISAC systems offer a new paradigm by simultaneously performing both sensing functionalities, such as radar, and communication functions using shared spectral and hardware resources. This approach maximizes spectral efficiency and reduces hardware implementation costs.

Driven by these compelling advantages, significant research efforts have been dedicated to designing ISAC systems in recent years [3], [4]. In [3], the authors proposed a beamforming design for ISAC systems that optimizes sensing performance in scenarios where communication and sensing-specific signals are simultaneously transmitted. However, this approach requires an advanced receiver capable of suppressing the dedicated sensing signal as interference, which is inconsistent with standard hardware assumptions. In [4], the authors proposed an index modulation technique employing frequency offset permutations to simultaneously improve communication throughput and sensing accuracy. Nevertheless, this approach demands a dedicated decoding mechanism beyond conventional fast Fourier transform (FFT)-based receivers and further depends on a non-standard transceiver architecture to implement hybrid beamforming in the terahertz band. Consequently, approaches relying on novel hardware architectures may encounter significant challenges in being integrated into existing communication standards.

Orthogonal frequency division multiplexing (OFDM), the dominant waveform in contemporary wireless networks, is well known for its advantages such as high spectral efficiency and strong robustness against multipath fading [5]. Moreover, OFDM technology enables simultaneous support for sensing, positioning, and communication functions, while fully utilizing existing communication infrastructure [6]. Building on these strengths, OFDM-based ISAC is actively being explored as a key component of future 6G systems [7]. In [8], a method was proposed in which a chirp signal is embedded into a conventional OFDM system to enable target range estimation without degrading communication performance. However, attaining high sensing performance in the considered monostatic radar environment requires hardware equipped with strong self-interference cancellation capabilities. In [9], the waveform was optimized to maximize both sensing and communication efficiency, using mutual information as a unified performance metric. However, this approach entails a non-trivial redesign of the waveform, making it incompatible with standard OFDM systems. While these studies highlight the considerable potential of OFDM-based ISAC, they also reveal critical limitations, such as increased hardware complexity and limited compatibility with standardized waveform architectures.

To overcome the aforementioned limitations, extensive research has been conducted on OFDM-ISAC systems that employ orthogonal sequences (OSs) compatible with standard communication protocols. In [10], an OFDM-ISAC system utilizing Zadoff–Chu (ZC) sequences as OSs was proposed. This system preserves compatibility with existing protocols by embedding a sensing sequence into one of the 14 OFDM symbols. However, its operation relies on the assumption of a persistent line-of-sight (LoS) path, which is often unrealistic in practical wireless environments such as urban scenarios. Meanwhile, [11] proposed an OFDM-ISAC algorithm for

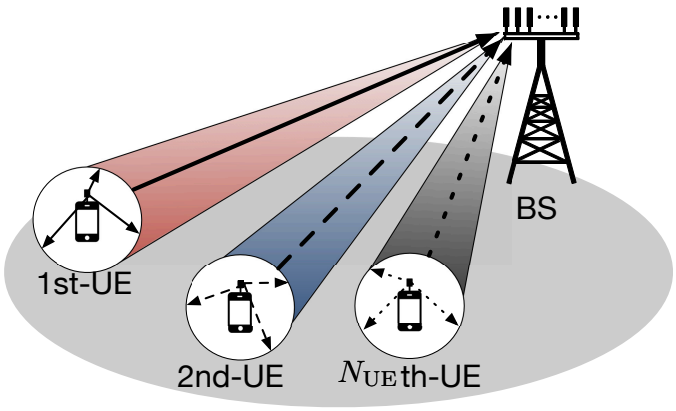

Fig. 1. System model of the proposed multi-User uplink ISAC in a multipath environment.

massive MIMO systems that exploits user-transmitted OS to improve channel estimation under non-line-of-sight (NLoS) conditions. Nevertheless, this scheme uses the sequences exclusively for sensing, while communication is carried out through conventional OFDM symbols, and thus falls short of achieving full integration in the strict sense of ISAC. The concept of true integration in ISAC refers to the simultaneous execution of communication and sensing functions using a single, unified waveform [12]. To pursue this objective, our previous work proposed an ISAC system in which a single user equipment (UE) transmits an OS to a base station (BS) for both localization and communication [13]. However, a key limitation of that study is its focus on a single-user scenario, whereas practical systems must inherently support multiple users.

In this paper, we extend the OFDM-ISAC system proposed in [13] to a multi-user scenario by introducing a sequence index grouping-based multiple access (SIGMA) technique. In the proposed method, OS indices are pre-assigned to each UE to ensure collision-free transmission, allowing all UEs to access the system and perform both communication and localization simultaneously. The communication bits are mapped to OS indices, and the BS, equipped with a uniform linear array (ULA), exploits the autocorrelation properties of the received OS to estimate the range and angle of arrival (AoA) of each UE. To capture a more realistic wireless environment, we adopt a local scattering channel model that accounts for the absence of LoS paths. Furthermore, to guarantee robust localization performance even in multipath environments, we introduce a clustering algorithm that jointly considers the estimated range, AoA, and received power. In addition, oversampling is applied to improve the resolution of range estimation and enhance overall sensing accuracy. The performance of the proposed OFDM-ISAC system is validated through extensive computer simulations, where communication performance is evaluated in terms of bit error rate (BER) and localization performance in terms of root mean squared error (RMSE).

II. System Model of Multi-User OFDM-ISAC

As illustrated in Fig. 1, we consider an uplink OFDM-ISAC system comprising N_{UE} single-antenna UEs and a BS equipped with a ULA of J elements. Without loss of generality, the BS is located at the origin (0,0) of the $x-y$ plane, while the $n \in \{1,\ldots,N_{\mathrm{UE}}\}$-th UE, UE$_n$, is positioned at $(d_n \cos\theta_n, d_n \sin\theta_n)$. Here, d_n is the distance and θ_n is the azimuth angle of UE$_n$ relative to the BS. We assume all nodes are stationary.

To model a realistic wireless environment, we adopt the local scattering channel model. This model presumes that the majority of scatterers are concentrated near the transmitter, a scenario that aligns well with the typical deployment of BSs on high-rise structure [11]. A feature of this model is that even in the absence of a LoS path, the multipath components arriving at the BS have AoA clustered around the nominal LoS direction [14]. This allows for the estimation of the user's position based on the geometric relationships within the channel, without relying on a direct LoS link. Under this model, we assume the signal propagates through L distinct multipath components. Consequently, in the considered multi-user environment, the signal received at the BS is the superposition of the signals transmitted from each UE, with each signal having propagated through its own unique channel.

In this paper, we propose OFDM-ISAC system where each UE transmits its communication data mapped to an OS. Although the most straightforward method to ensure robust performance would be to allocate orthogonal frequency resources to prevent inter-UE interference, using additional frequency bands is often impractical due to the scarcity and high cost of the spectrum. Therefore, to support multiple users within limited resources, we propose the SIGMA technique that partitions the available sequence with length N_{s} indices for bit stream transmission and allocates them to each UE. Specifically, a UE can transmit a maximum of $\lfloor \log_2 N_{\mathrm{s}} \rfloor$ bits by mapping its binary information to one of the available OS with length N_{s}. However, mapping the bit stream to all possible OS can lead to significant interference due to the effects of propagation and delay spread. To mitigate this, we define a candidate set of $M(=2^B)$ sequences to transmit B bits, where $B = \lfloor \log_2 (\lfloor N_{\mathrm{s}}/N_{\mathrm{CS}} \rfloor) \rfloor$. These sequences are generated by cyclically shifting the elements of a reference sequence $\mathbf{s}_0 \in \mathbb{C}^{N_{\mathrm{s}}}$ by integer multiples of N_{CS} samples. Specifically, the $m \in \{0,\ldots,N_{\mathrm{s}}-1\}$-th element of the $i \in \{0,\ldots,M-1\}$-th sequence, $\mathbf{s}_i$, is given by

$$s_i[m] = s_0\left[(m + iN_{\mathrm{CS}}) \bmod N_{\mathrm{s}}\right], \tag{1}$$

where mod denotes the modulo operator. Accordingly, the set of M candidate sequences is defined as $\mathcal{S} = \{\mathbf{s}_0, \mathbf{s}_1, \cdots, \mathbf{s}_{M-1}\}$. However, if multiple UEs transmit B bits simultaneously, sequence collisions can occur due to the shared candidate set, which can degrade the effective throughput. To prevent this, we distribute the entire set of M sequences evenly among the N_{UE} UEs, such that each UE uses $k = \lfloor M/N_{\mathrm{UE}} \rfloor$ sequences. Here, we assume that

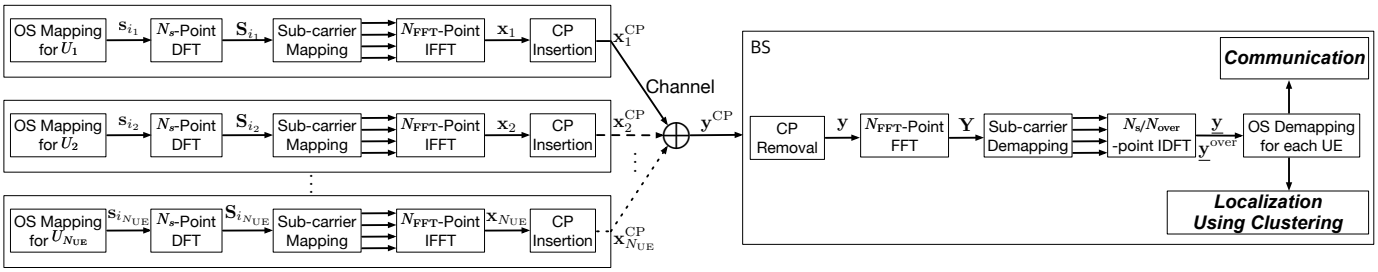

Fig. 2. Procedure of the proposed multi-user OFDM-ISAC Systems.

the BS knows the number of active UEs. In this case, each UE can transmit $B_{N_{\text{UE}}} = \lfloor \log_2 k \rfloor$ bits of data. Consequently, the n-th UE, where n is allocated the OS set $\mathcal{S}_n = \{\mathbf{s}_{(n-1)k}, \mathbf{s}_{(n-1)k+1}, \cdots, \mathbf{s}_{nk-1}\}$.

For clarity of explanation, we assume that the n-th UE transmits the i_n-th sequence $\mathbf{s}_{i_n}$, where $i_n \in \{(n-1)k, \ldots, nk-1\}$, which undergoes process depicted in Fig. 2. Since an OS such as ZC is typically defined in the time domain, it must be transformed into the frequency domain for OFDM subcarrier mapping via a discrete FT (DFT) of size N_{s}. The resulting frequency-domain signal mapped to the $v \in \{0, \ldots, N_{\text{s}}-1\}$-th subcarrier, $S_{i_n}[v]$, can be expressed as:

$$S_{i_n}[v] = \sum_{m=0}^{N_{\text{s}}-1} s_{i_n}[m] e^{-j2\pi \frac{v}{N_{\text{s}}} m}. \tag{2}$$

Subsequently, the UE performs an inverse FFT (IFFT) of size N_{FFT}, which is larger than N_{s}. The subcarriers corresponding to the difference between the FFT size and N_{s} are zero-padded. After the IFFT, the OS sample signal in the time domain at the $u \in \{0, \ldots, N_{\text{FFT}}-1\}$-th index, $x_n[u]$, is given by:

$$x_n[u] = \frac{1}{N_{\text{FFT}}} \sum_{v=0}^{N_{\text{FFT}}-1} S_{i_n}[v] e^{j2\pi \frac{v}{N_{\text{FFT}}} u}. \tag{3}$$

Then, a cyclic prefix (CP) of length N_{CP} is appended to (3), which can be expressed as:

$$x_n{}^{\text{CP}}[q] = x_n\left[(q - N_{\text{CP}}) \mod N_{\text{FFT}}\right], \tag{4}$$

where $x_n{}^{\text{CP}}[q]$ denotes the time-domain signal at the $q \in \{0, \ldots, N_{\text{FFT}} + N_{\text{CP}} - 1\}$-th index.

The signal received at the BS $j \in \{1, \ldots, J\}$-th antenna and the $g' \in \{0, \ldots, N_{\text{FFT}} + N_{\text{CP}} + L + \tau_j^{\max} - 2\}$-th time index, transmitted over L multipath channels, can be expressed:

$$y_j^{\text{CP}}[g'] = \sum_{n=1}^{N_{\text{UE}}} \sum_{l=0}^{L-1} \sqrt{d_{n,l}^{-\alpha}} h_{n,j}[l] x_n^{\text{CP}}\left[(g' - l - \tau_{n,j})\right] + z_j[g'], \tag{5}$$

where $\tau_{n,j}$ represents the number of samples corresponding to the propagation delay between the n-th UE and the j-th antenna of the BS and $\tau_j^{\max}$ represents the number of samples corresponding to the largest element of the propagation delay between the j-th antenna of the BS and all UEs. Also, $h_{n,j}[l]$ denotes the wireless channel vector for the $l \in \{0, \ldots, L-1\}$-th multipath component between the n-th UE and the j-th antenna of the BS, which can be expressed as:

$$h_{n,j}[l] = \beta_l e^{-j\frac{2\pi}{\lambda}(j-1)\Omega \cos(\theta_n + \Delta\theta_{n,l})}, \tag{6}$$

where λ is the wavelength, Ω is the antenna spacing, β_l is the complex channel gain following a normal distribution with zero mean and unit variance, $\theta_n \in [-\pi/2, \pi/2]$ is the AoA of the LoS path component, and $\Delta\theta_{n,l} \in [-\Delta\theta_{\max}, \Delta\theta_{\max}]$ represents the angular deviation of the l-th multipath component from the n-th UE [14]. The term $z_j[g]$ denotes the additive white Gaussian noise at the BS. In this paper, we assume perfect time synchronization between the BS and UEs, as proposed in [15]. Under the assumption that propagation delays are contained within the CP, the signal at the j-th antenna and the $g \in \{0, \ldots, N_{\text{FFT}} - 1\}$-th time index after CP removal can be expressed as:

$$y_j[g] = \sum_{n=1}^{N_{\text{UE}}} \tilde{h}_{n,j}[g] \circledast x_n\left[(g - \tau_{n,j}) \bmod N_{\text{FFT}}\right] + z_j[g], \tag{7}$$

where $\tilde{h}_{n,j}[g] \triangleq \sqrt{d_{n,l}^{-\alpha}} h_{n,j}[g]$ for $g = \{0, \ldots, L-1\}$ and otherwise $\tilde{h}_{n,j}[g] = 0$ By performing an FFT of size N_{FFT} on the CP-removed signal, the frequency-domain received signal is obtained as shown in (8). Here, $H_{n,j}$ and Z_j represent the results of performing a FFT of size N_{FFT} on $\tilde{h}_{n,j}$ and z_j, respectively. In (8), due to the zero-padding effect, the output for $\omega > N_{\text{s}} - 1$ generates negligibly small values.

To detect the transmitted sequence by leveraging the autocorrelation properties of the OS, the BS reconstructs the received signal in the time domain. An IDFT of size N_s is applied to the frequency-domain received signal Y_j. The resulting time-domain signal $\underline{y}_j(n)$ in the jth antenna can be approximated as:

$$\underline{y}_j[n] \approx \sum_{n=1}^{N_{\text{UE}}} \underline{h}_{n,j}[n] \circledast s_{i_n}\left[n - \left\lfloor \frac{N_{\text{s}}}{N_{\text{FFT}}} \tau_{n,j} \right\rfloor\right] + \underline{z}_j[n], \tag{9}$$

where $\circledast$ denotes the circular convolution operator, and the terms $\underline{h}_{n,j}$ and $\underline{z}_j$ represent the results of applying the IDFT of size N_{s} to the frequency-domain channel $H_{n,j}$ and noise Z_j, respectively.

$$Y_j[\omega] = \begin{cases} \sum_{n=1}^{N_{\text{UE}}} H_{n,j}[\omega] \cdot X_n[\omega] \cdot e^{-j\frac{2\pi\omega}{N_{\text{FFT}}}\tau_{n,j}} + Z_j[\omega], & \text{for } 0 \le \omega \le N_{\text{s}} - 1, \\ \text{FFT}\{y_j\}[\omega], & \text{for } \omega > N_{\text{s}} - 1. \end{cases} \tag{8}$$

III. Sequence Detection & Localization Procedure

This section describes how the BS can utilize the autocorrelation characteristics of the OS to detect the sequence transmitted by each UE, demodulate the communication bits, and estimate the location through oversampling and clustering.

A. Sequence Detection & Demodulation

The time-domain received signal, $\underline{y}_j$, preserves the transmitted sequence, which includes propagation delay information. Therefore, the BS calculates the autocorrelation between the multipath-affected received signal and a cyclically shifted version of the reference OS. The autocorrelation of the signal received at the j-th antenna of the BS can be calculated as:

$$R_j[\kappa] = \sum_{n=0}^{N_{\text{s}}-1} \underline{y}_j[n] s_0^*[n+\kappa], \tag{10}$$

where $*$ denotes the complex conjugate operator. The BS detects the candidate sequence transmitted by each UE via the peaks of the correlation profile. Since the OS candidates are distributed among the UEs in a non-overlapping manner, a detection window can be defined for each UE. The index of the peak correlation is then found within this user-specific window. The transmitted sequence index for the n-th UE at the j-th receive antenna, $\hat{i}_{n,j}$, is demodulated as follows:

$$\mathcal{C}_{n,j} = \arg\max_{\kappa \in \mathcal{K}_n} R_j[\kappa], \quad \hat{i}_{n,j} = \left\lfloor \frac{\mathcal{C}_{n,j}}{N_{\text{CS}}} \right\rfloor, \tag{11}$$

where $\mathcal{K}_n = \{(n-1)k \cdot N_{\text{CS}}, \ldots, (nk-1) \cdot N_{\text{CS}}\}$. Since the BS is equipped with J antennas, this process yields a set of detected indices $\{\hat{i}_{n,1}, \ldots, \hat{i}_{n,J}\}$. To leverage spatial diversity from the J receive antennas, the BS determines the final sequence index, $\hat{i}_n$, by selecting the mode of the per-antenna detected indices. The communication bits are then decoded using $\hat{i}_n$.

B. Estimation Location through Oversampling and Clustering

As seen in (9), even when using an OS, the correlation value may not peak at the exact index corresponding to the true propagation delay. Rounding errors from the IDFT/FFT size mismatch can cause a discrepancy between the correlation peak and the true propagation delay. Nevertheless, the distance can be estimate estimated from the peak index $\mathcal{C}_{n,j}$. Specifically, the distance between the j-th antenna of the BS and the n-th UE can be estimated based on (9) as:

$$\hat{d}_{n,j} = c \cdot T_s \cdot \frac{N_{FFT}}{N_s} \cdot \left(\mathcal{C}_{n,j} - \hat{i}_{n,j} \right), \tag{12}$$

where c is the speed of light and T_s is the sampling time. Therefore, the estimation resolution can be improved by inducing an oversampling effect, achieved by increasing the IDFT size used to reconstruct the time-domain sequence at the BS. By setting the IDFT size of $N_{\text{over}} (= \vartheta N_{\text{s}},\ \vartheta \in \mathbb{Z})$ as an integer multiple of the sequence length, the orthogonality of the sequence set is maintained. The correlation profile with oversampling can be expressed as:

$$R_j^{\text{over}}[\kappa] = \sum_{\zeta=0}^{N_{\text{over}}-1} \underline{y}_j^{\text{over}}[\zeta] \left(s_0^{\text{over}}\right)^* [\zeta + \kappa], \tag{13}$$

where $\underline{y}_j^{\text{over}}$ is the signal obtained by applying the IDFT of size N_{over} to Y_j, with the last $(N_{\text{over}} - N_{\text{FFT}})$ elements being zero-padded. Furthermore, the reference sequence $\mathbf{s}_0^{\text{over}} \in \mathbb{C}^{N_{\text{over}}}$ is a redefined. It is first transformed to the frequency domain via DFT and then transformed back to the time domain using the IDFT of size N_{over}. In this case, the cyclic shift value also increases proportionally to the oversampling ratio ϑ, becoming $N_{\text{CS}}^{\text{over}} = \vartheta N_{\text{CS}}$. Therefore, within the profile R_j^{over} allocated to the n-th UE, we first find the peak index $\mathcal{C}_{n,j}^{\text{over}} = \arg\max_{\kappa \in \mathcal{K}_n^{\text{over}}} R_j^{\text{over}}(\kappa)$,where $\mathcal{K}_n^{\text{over}} = \{(n-1)k \cdot N_{\text{CS}}^{\text{over}}, \ldots, (nk-1) \cdot N_{\text{CS}}^{\text{over}}\}$. And demodulate the sequence index as $\hat{i}_{n,j}^{\text{over}} = \left\lfloor \mathcal{C}_{n,j}^{\text{over}} / N_{\text{CS}}^{\text{over}} \right\rfloor$. The distance corresponding to this peak value $\mathcal{C}_{n,j}^{\text{over}}$ can then be calculated as follows:

$$\hat{d}_{n,j}^{\text{over}} = c \cdot T_s \cdot \frac{N_{\text{FFT}}}{N_{\text{over}}} \cdot \left(\mathcal{C}_{n,j}^{\text{over}} - \hat{i}_{n,j}^{\text{over}} \right). \tag{14}$$

Consequently, compared to the result in (12), the distance estimation resolution in (14) is improved by a factor of ϑ. Furthermore, since the oversampling process is performed in the digital signal processing domain, it can surpass the resolution limit imposed by the system bandwidth. We recognize that the distance estimate from each antenna can vary due to delay differences caused by their spatial separation. To address this, we designate the first antenna as the reference and adopt its estimated distance as the final value. This approach is chosen to minimize errors arising from the antenna array's geometry. Thus, the final estimated distance is given by $\hat{d}_n^{\text{over}} = \hat{d}_{n,1}^{\text{over}}$.

Subsequently, the direction of each UE is estimated using a correlation-based direction-finding algorithm, which has a relatively low computational complexity. Based on the estimated delay index for each antenna, $\mathcal{C}_{n,j}^{\text{over}}$, a despread signal in the spatial domain, $\mathbf{y}_n^{\text{over,des}} \in \mathbb{C}^J$, can be obtained. Specifically, the j-th element of $\mathbf{y}_n^{\text{over,des}}$ is calculated by correlating the oversampled time-domain received signal vector, $\underline{y}_j^{\text{over}}$, with the reference sequence corresponding to the estimated index $\mathcal{C}_{n,j}^{\text{over}}$. Next, we define a sensing matrix $\mathbf{A} \in \mathbb{C}^{J \times P}$ composed of steering vectors corresponding to P possible AoA. The value of P is determined by the desired angular resolution. For example, if the BS is equipped with a ULA and the AoA search range is $[-90^\circ, 90^\circ]$ with a 1° resolution, the

first column of $\mathbf{A}$, denoted as $\mathbf{a}_1 \in \mathbb{C}^J$, would represent the steering vector for an AoA of -90°. Using the despread signal, the direction can be estimated by identifying the index that yields the maximum correlation with the sensing matrix, as follows:

$$\hat{p}_n^{\text{over}} = \arg \max_{p \in \{1,\ldots,P\}} \left| \mathbf{a}_p^H \mathbf{y}_n^{\text{over,des}} \right|, \tag{15}$$

where $\mathbf{a}_p \in \mathbb{C}^J$ is the p-th column of the sensing matrix. The estimated index $\hat{p}_n^{\text{over}}$ can then be converted to the final estimated angle, $\hat{\theta}_n^{\text{over}}$, for the n-th UE.

If a LoS path were available, the position of the n-th UE could be estimated directly using $\hat{d}_n^{\text{over}}$ and $\hat{\theta}_n^{\text{over}}$. However, as this paper considers multipath environments, we introduce the density-based spatial clustering of applications with noise (DBSCAN) technique for more robust localization [16]. First, for the localization of the n-th UE, we collect a set of measurements for each potential path. The estimated distances, angles, and received powers corresponding to the path indices in the set $\mathcal{F}_n = \{\hat{i}_{n,j}^{\text{over}}, \ldots, \hat{i}_{n,j}^{\text{over}} + N_{\text{CS}}^{\text{over}} - 1\}$ are stored in the vectors $\mathbf{d}_{n,1} \in \mathbb{R}^{N_{\text{CS}}^{\text{over}}}$, $\mathbf{d}_{n,2} \in \mathbb{R}^{N_{\text{CS}}^{\text{over}}}$, and $\mathbf{d}_{n,3} \in \mathbb{R}^{N_{\text{CS}}^{\text{over}}}$, respectively. We perform feature scaling to prevent features with larger numerical ranges from dominating the clustering algorithm. Specifically, we apply Z-score normalization to each column $\mathbf{d}_{n,\gamma}$ of the data matrix $\mathbf{D}_n = [\mathbf{d}_{n,1}\ \mathbf{d}_{n,2}\ \mathbf{d}_{n,3}]$ using the expression:

$$\tilde{\mathbf{d}}_\gamma = (\mathbf{d}_\gamma - \mathbb{E}[\mathbf{d}_\gamma])/\sigma_{\mathbf{d}_\gamma}, \tag{16}$$

where $\mathbb{E}[\mathbf{d}_\gamma]$ and $\sigma_{\mathbf{d}_\gamma}$ represent the mean and standard deviation of the corresponding feature. As a pre-filtering step to enhance computational efficiency, we first discard any data points whose normalized received power, $\tilde{\mathbf{d}}_{n,3}$, falls below a predefined threshold, η. The DBSCAN algorithm is then applied to the remaining data points. The resulting cluster containing the largest number of members is identified as the one corresponding to the desired signal from the n-th UE. We denote the set of points in this dominant cluster as $\mathcal{D}_n$ and construct a new matrix $\bar{\mathbf{D}}_n \in \mathbb{R}^{|\mathcal{D}_n| \times 3}$ from these points. Finally, the estimates for the n-th user's distance and angle are derived from this selected cluster. The final n-th UE distance $\hat{d}_n^{\text{fin}}$ is determined by the minimum distance value within the cluster. The final n-th UE angle $\hat{\theta}_n^{\text{fin}}$ is calculated as the arithmetic mean of all angles in the cluster, providing a robust central estimate. This is expressed as:

$$\hat{d}_n^{\text{fin}} = \min_{\varsigma \in \{1,\ldots,|\mathcal{D}_n|\}} \bar{d}_{n,\varsigma 1}, \quad \hat{\theta}_n^{\text{fin}} = \frac{1}{|\mathcal{D}_n|} \sum_{\varsigma=1}^{|\mathcal{D}_n|} \bar{d}_{n,\varsigma 2}, \tag{17}$$

where $\bar{d}_{n,ij}$ is the element in the i-th row and j-th column of the cluster matrix $\bar{\mathbf{D}}_n$.

IV. Simulation Results

In this section, we evaluate and analyze the communication and positioning performance of the proposed multi-user OFDM-ISAC system through Monte Carlo simulations implemented in MATLAB. We model the multipath environment based on the tapped delay line (TDL)-B model defined in 3GPP TR 38.901, applying scaling factors corresponding to the short delay profile scenario for an urban microcell (UMi) street-canyon environment. The simulation parameters, including the angular spread for a local scattering environments, are summarized in Table I. We generate a set of $M = 64$ candidate sequences to be used as OS by setting the ZC sequence parameters to $N_{\text{s}} = 839$ and $N_{\text{CS}} = 13$. The n-th UE is assumed to be located at the polar coordinates $(d_n \cos\theta_n, d_n \sin\theta_n)$, where the position is defined by $d_n = 40 + 5(n-1)$ meters and $\theta_n = 40^\circ + 5^\circ(n-1)$. For accurate range and angle detection, our simulation performs clustering on $5N_{\text{CS}}^{\text{over}}$ data samples collected over five sequences, a process that takes only 136.76 μs. This short acquisition period is achieved without degrading communication throughput, as the transmitted bits are updated in each sub-block.

TABLE I
Simulation Parameters

Parameter	Value	Parameter	Value
Center frequency (f_c)	1.8 GHz	Maximum angle deviation ($\Delta\theta_{max}$)	5°
FFT size (N_{FFT})	2048	CP size (N_{CP})	256
Threshold value (η)	1	Path loss exponent (α)	2
Sampling time (T_s)	32.6 ns	Subcarrier spacing (Δf)	15 kHz

Fig. 3 shows the average BER performance versus the energy-per-bit to noise ratio, E_b/N_0, for a varying N_{UE}. The baseline method assumes that all UEs share the same candidate set, and the BS detects the N_{UE} indices corresponding to the strongest correlation peaks [13]. The results demonstrate that our proposed system outperforms the baseline in all multi-user scenarios. The slight performance degradation observed as the number of UEs increases is attributable to the reduced sequence pool available to each user. A smaller allocation heightens the probability of a UE selecting a sequence near a partition boundary, thus increasing the risk of misdetection due to interference from adjacent user sets.

Fig. 4 illustrates the average RMSE performance for all UEs as a function of the E_b/N_0 for a varying N_{UE}. The RMSE of the n-th UE's estimated position is defined as follows:

$$\text{RMSE}_n = \sqrt{\mathbb{E}\left[\left(\hat{d}_n \cos\hat{\theta}_n - d_n \cos\theta_n\right)^2 + \left(\hat{d}_n \sin\hat{\theta}_n - d_n \sin\theta_n\right)^2\right]}. \tag{18}$$

The results show that position estimation is feasible even without a LoS path. Furthermore, when oversampling is applied with $\vartheta = 8$, the positioning performance is superior to the non-oversampled, $\vartheta = 1$, case due to the enhanced range estimation resolution. Specifically, at high E_b/N_0, the positioning RMSE for the oversampled case saturates at approximately 4.5m, independently of N_{UE}. In conclusion, we have demonstrated that the proposed OFDM-ISAC system can ensure both communication and sensing performance using the same wireless resources and hardware, without requiring significant modifications to the existing OFDM system architecture.

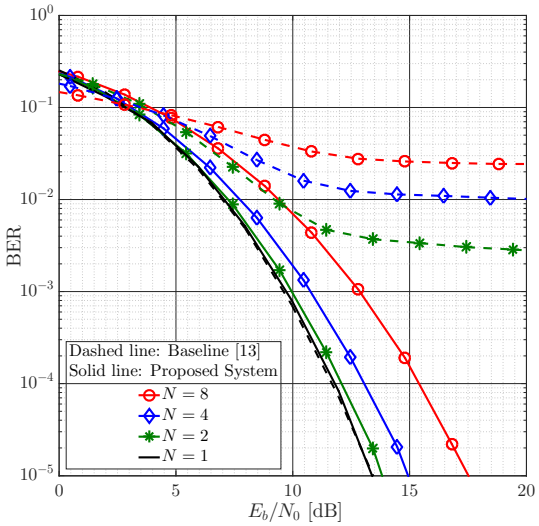

Fig. 3. BER performance comparison in the proposed multi-user OFDM-ISAC system under different numbers of active users.

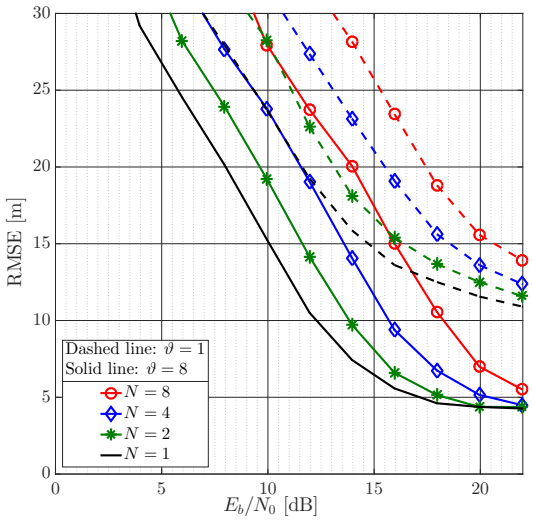

Fig. 4. RMSE performance comparison in the proposed multi-user OFDM-ISAC system with and without oversampling under different numbers of active users.

V. Conclusion

In this paper, we propose a novel sequence index grouping-based multiple access (SIGMA) technique for the multi-user orthogonal frequency division multiplexing (OFDM)-based integrated sensing and communication (ISAC) system. The proposed technique orthogonally distributes sets of orthogonal sequences (OS) to each user equipment (UE) and utilizes index modulation and autocorrelation properties to perform both communication and sensing functions. Furthermore, by incorporating oversampling and a clustering algorithm at the signal processing stage, the system can effectively estimate user positions even in multipath environments. Simulation results demonstrate that the proposed technique is compatible with the conventional OFDM waveform and maintains robust communication and sensing performance in multi-user scenarios.

Acknowledgment

This research was supported in part by the National Research Foundation of Korea (NRF) grant funded by the Korea Government (MSIT) (No. RS-2025-02303435) and in part by the National Research Foundation of Korea (NRF) grant funded by the Korea Government (MSIT), Research on Interdisciplinary Wireless Communication Technology for IntraTube High-Speed Mobility (No. RS-2024-00420013).

References

[1] K. Raheel *et al.*, "Design and performance evaluation of orthogonally polarized corporate feed MIMO antenna array for next-generation communication system," *IEEE Access*, vol. 12, pp. 30382–30397, Feb. 2024.

[2] Y. Jiang *et al.*, "Integrated sensing and communication for low altitude economy: Opportunities and challenges," *IEEE Commun. Mag.*, Early Access, pp. 1–7, Apr. 2024.

[3] H. Hua, J. Xu, and T. X. Han, "Optimal transmit beamforming for integrated sensing and communication," *IEEE Trans. Veh. Technol.*, vol. 72, no. 8, pp. 10588–10603, Aug. 2023.

[4] J. Jian, Q. Huang, B. Huang, and W. -Q. Wang, "FDA-MIMO-based integrated sensing and communication system with frequency offsets permutation index modulation," *IEEE Trans. Commun.*, vol. 72, no. 11, pp. 6707–6721, Nov. 2024.

[5] M. S. J. Solaija, S. E. Zegrar, and H. Arslan, "Orthogonal frequency division multiplexing: The way forward for 6G physical layer design?," *IEEE Veh. Technol. Mag.*, vol. 19, no. 1, pp. 45–54, Jan. 2024.

[6] F. Zhang *et al.*, "Cross-domain dual-functional OFDM waveform design for accurate sensing/positioning," *IEEE J. Sel. Areas Commun.*, vol. 42, no. 9, pp. 2259–2274, Sep. 2024.

[7] C. Han, Y. Wu, Z. Chen, Y. Chen, and G. Wang, "THz ISAC: A physical-layer perspective of terahertz integrated sensing and communication," *IEEE Commun. Mag.*, vol. 62, no. 2, pp. 102–108, Feb. 2024.

[8] W. Cho, K. Chang, W. Shin, Y. Kim, and Y. -J. Ko, "OFDM-based in-band full-duplex ISAC systems," *IEEE Wireless Commun. Lett.*, vol. 14, no. 2, pp. 365–369, Feb. 2025.

[9] Z. Wei *et al.*, "Waveform design for MIMO-OFDM integrated sensing and communication system: An information theoretical approach," *IEEE Trans. Commun.*, vol. 72, no. 1, pp. 496–509, Jan. 2024.

[10] M. Wang, K. Yoshii, S. Shimamoto, M. Funakoshi, A. Yabuki, and H. Funayoshi, "An OFDM-ISAC scheme based on Zadoff-Chu sequence For 5G NR base-station," in *Proc. IEEE Consum. Commun. Netw. Conf. (CCNC)*, Las Vegas, NV, USA, 2025.

[11] K. Xu, X. Xia, C. Li, C. Wei, W. Xie, and Y. Shi, "Channel feature projection clustering based joint channel and DoA estimation for ISAC massive MIMO OFDM system," *IEEE Trans. Veh. Technol.*, Vol. 73, no. 3, pp. 3678–3689, Mar. 2024.

[12] J. Du *et al.*, "An overview of resource allocation in integrated sensing and communication," in *Proc. IEEE Int. Conf. Commun. China (ICCC) Workshops*, Dalian, China, 2023.

[13] H. -E. Lee, Y. -S. Lee, and B. C. Jung, "Off-the-shelf OFDM-ISAC system with clustering algorithm for multipath environments," in *Proc. IEEE Wireless Commun. Netw. Conf. (WCNC)*, Italy, Milan, 2025.

[14] E. Björnson, J. Hoydis, and L. Sanguinetti, "Massive MIMO networks: Spectral, energy, and hardware efficiency," *Found. Trends Signals Process.*, vol. 11, pp. 154–655, Nov. 2017.

[15] H. Minn, V. K. Bhargava, and K. B. Letaief, "A robust timing and frequency synchronization for OFDM systems," *IEEE Trans. Wireless Commun.*, vol. 2, no. 4, pp. 822–839, Jul. 2003.

[16] M. Ester, H. P. Kriegel, J. Sander, and X. Xu, "A density-based algorithm for discovering clusters in large spatial databases with noise," in *Proc. KDD.*, Portland, OR, USA, 1996, pp. 226–231.